

AUTHOR QUERIES

AUTHOR PLEASE ANSWER ALL QUERIES

PLEASE NOTE: Please note that we cannot accept new source files as corrections for your article. If possible, please annotate the PDF proof we have sent you with your corrections and upload it via the Author Gateway. Alternatively, you may send us your corrections in list format. You may also upload revised graphics via the Author Gateway.

Carefully check the page proofs (and coordinate with all authors); additional changes or updates WILL NOT be accepted after the article is published online/print in its final form. Please check author names and affiliations, funding, as well as the overall article for any errors prior to sending in your author proof corrections. Your article has been peer reviewed, accepted as final, and sent in to IEEE. No text changes have been made to the main part of the article as dictated by the editorial level of service for your publication.

AQ:1 = Please confirm or add details for any funding or financial support for the research of this article. **Removed Grant RTI2018-098116-B-C22**

AQ:2 = Please confirm that the human and animal research disclosure statement is correct as set. **Correct**

AQ:3 = If you haven't done so already, please make sure you have submitted a graphical abstract for your paper. The GA should be a current figure or image from your accepted article. The GA will be displayed on your articles abstract page on IEEE Xplore. Please choose a current figure from the paper and supply a caption at your earliest convenience for the graphical abstract. Note that captions cannot exceed 1800 characters (including spaces). If you submitted a video as your graphical abstract, please make sure there is an overlay image and caption. Overlay images are usually a screenshot of your video that best represents the video. This is for readers who may not have access to video-viewing software. Please see an example in the link below: <http://ieeaccess.ieee.org/submitting-an-article/>
The GA is already submitted.

AQ:4 = Please confirm the retention of the content in the acknowledgement section. **Please, separate the "Acknowledgment" section from the "Author Contributions"**

AQ:5 = The term "Chairman" may be considered non-inclusive. Please consider using "Chairperson" instead. **Replace "Chairman" by "Chairperson"**

AQ:6 = Author photos appear to be too blurry. Please provide a better

quality/higher image for the author JAVIER ROSELL.



Received 20 August 2022, accepted 21 September 2022. Date of publication 00 xxxx 0000, date of current version 00 xxxx 0000.

Digital Object Identifier 10.1109/ACCESS.2022.3209809

Effect of Calibration for Tissue Differentiation Between Healthy and Neoplasm Lung Using Minimally Invasive Electrical Impedance Spectroscopy

GEORGINA COMPANYY-SE¹, LEXA NESCOLARDE¹, VIRGINIA PAJARES², ALFONS TORREGO², PERE J. RIU¹, (Senior Member, IEEE), JAVIER ROSELL¹, (Senior Member, IEEE), AND RAMON BRAGÓS¹

¹Department of Electronic Engineering, Universitat Politècnica de Catalunya, 08034 Barcelona, Spain

²Department of Respiratory Medicine, Hospital de la Santa Creu i Sant Pau, 08041 Barcelona, Spain

Corresponding author: Lexa Nescolarde (lexa.nescolarde@upc.edu)

This work was supported in part by the Spanish Ministry of Science and Innovation under Grant RTI2018-098116-B-C21 and Grant RTI2018-098116-B-C22; in part by the Secretariat of Universities and Research of the Generalitat de Catalunya and the European Social Fund developed in the Electronic and Biomedical Instrumentation Research Group of the Electronic Engineering Department, Universitat Politècnica de Catalunya; and in part by the Interventional Pulmonology Unit of the Respiratory Medicine Department of the Hospital de la Santa Creu i Sant Pau, Barcelona, Spain.

This work involved human subjects or animals in its research. Approval of all ethical and experimental procedures and protocols was granted by the Ethics Committee on Clinical Investigation of the Hospital de la Santa Creu i Sant Pau, Barcelona, Spain, under Application No. CEIC-73/2010.

ABSTRACT This study proposes a calibration method and analyses the effect of this calibration in lung measures, using minimally invasive electrical impedance spectroscopy with the 3-electrode method, for tissue differentiation between healthy and neoplasm lung tissue. Tissue measurements were performed in 99 patients [54 healthy tissue and 15 neoplastic tissue samples obtained] with an indicated bronchoscopy. Statistically significant difference ($P < 0.001$) were found between healthy lung tissue and neoplasm lung tissue in bioimpedance parameters. The calibration of the bioimpedance measures with respect to a measure performed in bronchi reduces the inter-patient dispersion, increasing the sensitivity, decreasing the specificity and increasing the area below the ROC curve for three out of four impedance-derived estimators. Results also show that there are no significant differences between healthy lung tissue among smoker, non-smoker and ex-smoker samples, which was initially stated as a possible cause of EIS measurement dispersion in lungs.

INDEX TERMS Bronchi, bronchoscopy, calibration, electrical impedance spectroscopy (EIS), lung.

I. INTRODUCTION

Respiratory disorders have a big impact in the population worldwide. According to the European Respiratory Society, chronic obstructive pulmonary disease (COPD) is the third global cause of death in more developed countries. Moreover,

The associate editor coordinating the review of this manuscript and approving it for publication was Norbert Herencsar¹.

lung cancer is the leading cause of cancer death in the world. Both are smoking-related conditions [1].

In lung cancer, late detection in advance stages is common and is related to poor prognosis [2]. Diagnostic of lung peripheral and central nodules is increasing because of number of patients with indeterminate nodules are discovered in CT screening and verified with other diagnostic options such as minimally invasive bronchoscopic procedures to establish final histological type. However, the diagnostic yield using

27 virtual bronchoscopy (VB), radial endobronchial ultrasound
28 (r-EBUS), electromagnetic navigation (EMN) and ultrathin
29 bronchoscopes remains suboptimal [3], [4], and their high
30 economic cost makes them unavailable in most centers.

31 We aim to use Electrical Impedance Spectroscopy (EIS) to
32 complement the actual methods of diagnosis of lung diseases
33 as it could allow the differentiation between healthy lung
34 tissue and neoplasm lung tissue and help in the choice of the
35 specific sample location.

36 EIS technique is one of the existing methods of impedance
37 analysis. Impedance is defined as the opposition to the flow of
38 an alternating electrical current which is dependent on the fre-
39 quency of this current [5]. When the impedance is measured
40 in biological tissue is named as bioimpedance (Z). It measures
41 the passive electrical properties of the tissue after the intro-
42 duction of a low amplitude alternating current to the organism
43 [5], [6]. The bioimpedance is a complex number with a real
44 part (the resistance, R) and an imaginary part (the reactance,
45 X_c), both parts are dependent of the geometry of the mea-
46 sured region, the location of electrodes and the tissue elec-
47 trical passive properties [5]. The physiological fluids have
48 low resistance and dominates the measured resistance, while
49 cell membranes act as capacitors, having high impedance
50 at low frequencies and low impedance at high frequencies
51 and contributes mainly to the reactive part. Due to these
52 behaviors, the electrical current introduced in the biological
53 tissue divides into resistive and capacitive pathways and it
54 changes with the frequency [6]. An alternative representation
55 of the Bioimpedance, as a complex number, is the use of the
56 modulus (Z) and the phase angle (PA). The PA represents
57 the relative time lag between the injected current and the
58 generated voltage [7]. Bioimpedance data can be obtained
59 using single or multiple frequencies. When the bioimpedance
60 data is obtained using a broad band of frequencies is known
61 as bioimpedance spectroscopy [6]. The advantage of the EIS
62 method, to measure and analyze bioimpedance data, is based
63 on the fact that current at low frequency (lower than 10 kHz)
64 flows through the extracellular medium while current at high
65 frequencies (over 100 kHz) flows through both, intracellular
66 and extracellular medium, giving more information about the
67 structure of the tissue.

68 There are previous studies about lung bioimpedance mea-
69 surements. Toso *et al.* [8], through an impedance plethysmo-
70 graph emitting 50 kHz alternating current, reported different
71 impedance vector distribution in patients with lung cancer
72 as compared with healthy patients. A reduced X_c and a
73 smaller PA were found while R was preserved in patients
74 with lung cancer. Nierman *et al.* [9] performed transthoracic
75 bioelectrical impedance analysis to quantify extravascular
76 lung water in animal models. Orschulik *et al.* [10] used
77 non-invasive bioimpedance spectroscopy for the diagnosis of
78 acute respiratory distress syndrome in an animal model.

79 Some previous studies have been carried out by our
80 research group. Sanchez *et al.* [11] performed minimally
81 invasive lung bioimpedance measurements to study the char-
82 acteristics of lung bioimpedance (calibration and linearity)

and the differences between inflated and deflated lung. Later
Coll *et al.* [12] and Riu *et al.* [13] present studies demonst-
rating the potential for tissue differentiation through minimally
invasive electrical impedance spectroscopy in lung using the
4-electrode method.

This manuscript (2nd phase) is the continuation of the pre-
vious study (1st phase) entitled “Minimally invasive lung tis-
sue differentiation using electrical impedance spectroscopy:
a comparison of the 3- and 4- electrode methods” performed
by Company-Se *et al.* [14]. It compared the capacity of tissue
differentiation of the minimally invasive electrical impedance
spectroscopy in lungs using the 4-electrode method and the
3-electrode method. The results showed that both meth-
ods were adequate for tissue differentiation but 3-electrode
method was more feasible for its clinical use because of its
lower complexity, both in the catheter configuration (single
electrode) and in the measurement system architecture. This
previous study proposed for future works to increase the
sample size for the differentiation between healthy lung tissue
and neoplasm lung tissue using the 3-electrode method.

In this 2nd phase the measures performed in healthy lung
tissue and in neoplasm lung tissue showed high inter-patient
variability. This variability could hinder the tissue differenti-
ation in lungs. There are several causes for this variability:
1) The measured absolute values of the R and X_c spectra
are influenced by the tissue properties (the variable under
measurement) but also by the geometry of the measurement
(body shape of the patient and electrode positions). Geometrical
factors such as body mass index (BMI) has been reported
as one significant factor for changes in lung metrics [15];
2) The breathing produces also impedance changes due to the
considerable air volume change from inspiration to expiration
and the influence of the non-conductive air contents in the
lung tissue. This phenomenon could increase the inter-patient
variability as depending on the patient, the breathing cycle
will be different; 3) In the 3-electrode method, the electrode
impedance of the catheter tip is measured and could increase
the intra- and inter-patient variability due to poor contact
of the catheter tip against the lung tissue and the liquids
accumulation in the airways; 4) Another potential cause for
inter-patient variability is cigarette consumption. It could
contribute to the increase of the inter-patient dispersion.
Smoking-induced epithelial abnormalities can serve both as
targets for abnormal inflammatory responses and as initia-
tors of deregulated inflammation. Cytokines, chemokines,
and growth factors released by alveolar macrophages, lym-
phocytes, neutrophils, endothelial cells, and fibroblasts
may act to promote epithelial dysfunction and malignant
progression [16], [17].

While the ventilation-induced impedance modulation
effect can be reduced using averaging, the other potential
causes of variability need a calibration method capable to
reduce this variability in order to perform tissue differ-
entiation with success. For example, electrical impedance
measures using the 3-electrode method in cardiology uses
a floating measure within the heart (catheter completely

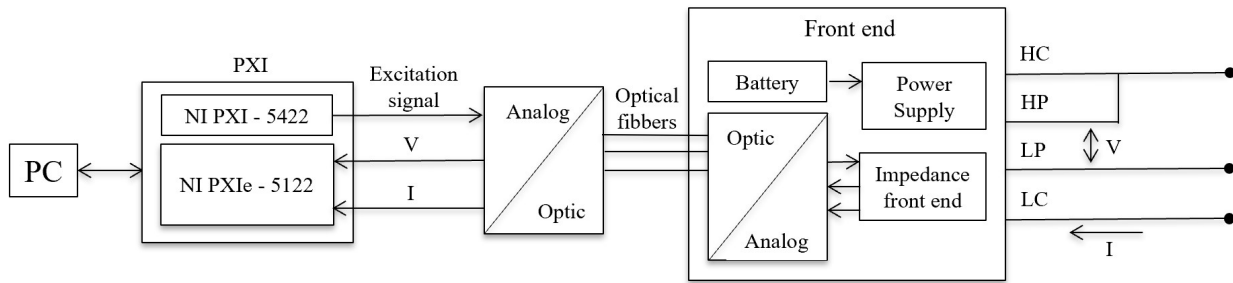


FIGURE 1. Schematic representation of the bioimpedance acquisition system.

surrounded by blood) to calibrate the geometrical factors in the bioimpedance measures obtained in contact with the myocardial walls [18], and also, partially, the electrode impedance effect. In lungs, a floating measure completely surrounded by air to calibrate is not viable due to the non-conductive property of the air and it is not feasible to locate the catheter in a place where the tip electrode will be surrounded by a well-known tissue and which will be affected by geometrical factors similar to the ones that will affect the tissue impedance measurements for each patient. For this reason, we proposed to acquire a bioimpedance measure in principal bronchus and use it to calibrate the lung tissue bioimpedance measures.

The aim of this study, by using minimally invasive electrical impedance spectroscopy with the 3-electrode method, is to propose a calibration method and to analyze the effect of this calibration in measures performed in the bronchi for tissue differentiation in different groups: healthy lung tissue (no radiological abnormalities in CT Thorax) and neoplasm lung tissue. Also, the possible differences in the impedance measurements in healthy tissue in smokers, non-smokers and ex-smokers will be verified to check if this factor would affect the ability to differentiate between healthy lung tissue and lung neoplasm.

II. MATERIALS AND METHODS

A. PARTICIPANTS

Minimally invasive EIS measures were taken in 99 patients (Age: 65 ± 16 yr; Weight: 76.8 ± 15.6 kg; BMI: 27.7 ± 5.5 kgm^{-2}) with a bronchoscopy indicated during the period between November 2021 and February 2022 at the “Hospital de la Santa Creu i Sant Pau”. All of them underwent bioimpedance measurement. However, 30 of them had other characteristics than healthy lung tissue or neoplasm lung tissue such as emphysema or fibrosis. For this reason, out of the 99 patients measured by bioimpedance, only 69 were considered for analysis (healthy: 54 and neoplastic: 15).

The number of bioimpedance samples obtained in healthy lung tissue were 54 [(non-smokers: $n = 22$, Age: 59 ± 19 yr; Weight: 70.8 ± 16.6 kg; BMI: 26.7 ± 5.8 kgm^{-2}); smokers: $n = 9$, Age: 66 ± 7 yr; Weight: 83.5 ± 11.9 kg; BMI:

31.0 ± 4.3 kgm^{-2}); (ex-smokers: $n = 23$, Age: 71 ± 12 yr; Weight: 79.3 ± 13.8 kg; BMI: 27.5 ± 4.8 kgm^{-2} ; years without smoking = 22 ± 11 yr)] while the number of samples obtained from neoplasm lung tissue were 15 (Age: 70 ± 9 yr; Weight: 75.3 ± 11.2 kg; BMI: 26.3 ± 4.1 kgm^{-2}).

Ethics approval was obtained from the Hospital de la Santa Creu i Sant Pau (CEIC-73/2020) according to principles of the Declaration of Helsinki for experiments with human beings. All patients proved signed informed consent.

B. MEASUREMENT SYSTEM

The acquisition of bioimpedance measures were performed using a tetrapolar catheter (Medtronic 5F RF Marinr), 115 cm long with a diameter of 1.65 mm (5 F) and two skin electrodes (Ambu BlueSensor VLC ref: VLC-00-s/10 and 3M Company ref: 9160F) placed on the right side of the patients at the level of the ribs. Only the catheter tip electrode will be used in the measurements.

The measurement system is made up of 3 devices (Fig. 1): 1) an optically insulated battery-powered patient interface insulated front end (that includes the impedance front end); 2) a rugged PC platform based on a PXI system from National Instruments; and 3) an analog-optical interface front-end to connect the PXI with the insulated front end. An arbitrary waveform generator generates a multisine excitation signal that is composed of 26 frequencies between 1 kHz and 1 MHz. To ensure a current lower than the maximum allowable patient auxiliary current established in the IEC 60601-1:2005 ($<1\text{mA}$ rms measured with the circuit proposed in the IEC 60601-1:2005) the front end includes an AC-coupled current source that attenuates the low-frequency components accordingly with the current limit pattern specified by this standard. The system was verified including the 26 frequency components (1 kHz – 1MHz) simultaneously.

The voltage ($V(t)$) and current ($I(t)$) are simultaneously acquired. Then, with the optical-analog interface connected to the PXI, the excitation is converted into an optical signal. The optical signal is then converted back into an electrical signal inside the front end. The voltage and current signals, optically transmitted from the front end to the optical-electrical interface, are acquired with the digitizer card. The acquisition

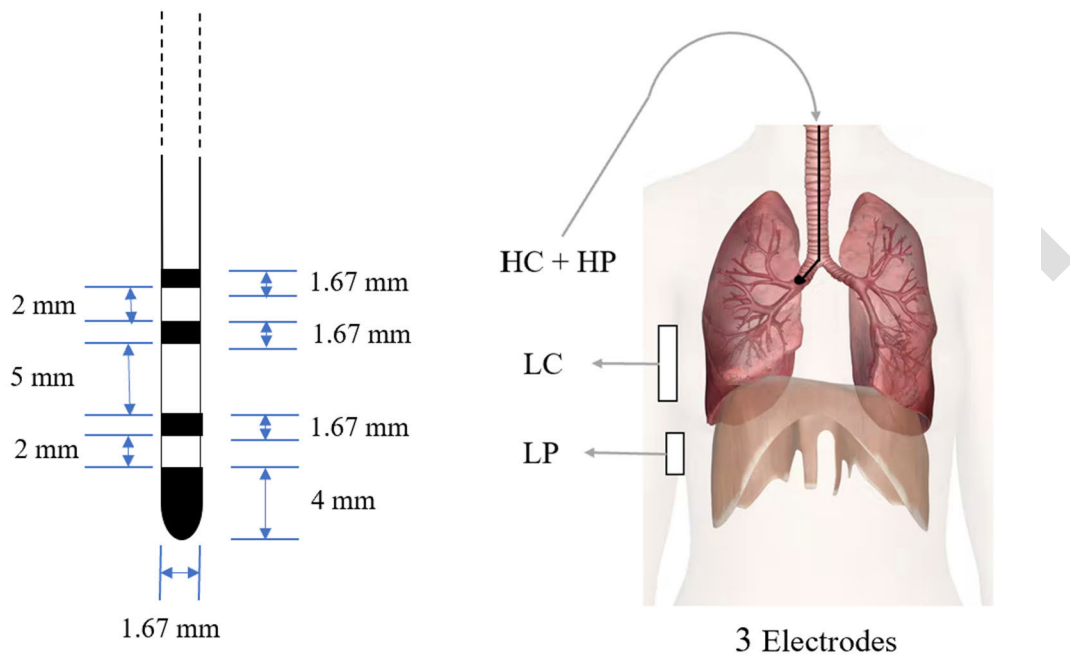


FIGURE 2. Right figure: Schematic representation of the 3-electrode method. In the 3-electrode method the LC and LP electrodes are placed on the skin using skin surface electrodes. Left figure: dimensions of the catheter. Only the tip electrode of the catheter is used to perform the measurements.

219 system takes simultaneous samples of voltage and current
 220 at 20 MSamples/s. From the acquired signals, 60 impedance
 221 spectra per second are obtained.

222 Bioimpedance measures were obtained using the
 223 3-electrode method. To inject the current (HC) and detect the
 224 potential (HP) the electrode located at the tip of the catheter
 225 is used. The two skin electrodes are used as low current (LC)
 226 and loc potential (LP) electrodes (Fig. 2).

227 C. MEASUREMENT PROTOCOL

228 Bronchoscopy, a procedure used to inspect the airways, was
 229 performed to obtain the bioimpedance measures. As part of
 230 the diagnostic process, radiological imaging technique (CT
 231 or PET/CT) were performed in each patient before bron-
 232 choscopy procedure. To obtain the bioimpedance measures,
 233 the catheter was inserted through a port of the bronchoscope.
 234 During the bronchoscopy, patients are placed in a supine
 235 position with the upper airways anaesthetized with topical 2%
 236 lidocaine. Moreover, intravenous sedation is provided with
 237 midazolam, fentanyl and propofol. During the process, mea-
 238 sures in bronchial tissue, healthy lung tissue and neoplasm
 239 lung tissue, if applicable, were taken. The acquisition of the
 240 measures had a duration of 12 seconds.

241 D. EIS MEASUREMENTS

242 To obtain the EIS measurements the system applies a mul-
 243 tisine current signal and acquires the voltage and current
 244 signals. The Fast Fourier Transform (FFT) is used to obtain

the ratio between the voltage and current coefficients of the
 FFT corresponding to each injected frequency.

245
 246
 247 The acquisition takes 12 s at 60 spectra per second. The 3-
 248 electrode measurements were calibrated with a measurement
 249 over a known resistor (600 Ohms) connected to the catheter
 250 tip and to the external electrode connectors.

251 E. CALIBRATION USING BRONCHUS

252 To remove the geometrical factors of the patients a multi-
 253 plicative factor calibration of the bioimpedance of the lung
 254 measures is proposed. The proposed method aims to calibrate
 255 the lung measures with respect to a measure performed in
 256 the bronchial tissue (principal bronchus) for each respec-
 257 tive patient. A measurement in the bronchi is of no interest
 258 in clinical practice, therefore, impedance measurement in
 259 bronchial tissue offers the advantage of calibration while
 260 not losing relevant clinical information. Moreover, because
 261 of its low cell content, bronchial tissue should have a flat
 262 impedance spectrum, thus being suitable as calibration refer-
 263 ence [14]. The obtained impedance modulus ($|Z|$) of the lung
 264 is divided by the mean value (mean value of impedance at
 265 each frequency, during a time interval) of $|Z|$ of the bronchial
 266 tissue and then multiplied by a factor of 100Ω , which is the
 267 expected impedance magnitude value obtained in the bronchi
 268 [12] (1). The PA calibrated of the lung measure is obtained by
 269 subtracting the original value of the PA of the lung measure
 270 minus the mean value of the PA obtained in the bronchi tissue

271 sample (2).

$$272 \quad |Z(f, t)|_{calibrated} \\ 273 \quad = 100 * |Z(f, t)|_{lung} / mean(|Z(f, t)|_{bronchi}) \quad (1)$$

$$274 \quad PA_{calibrated}(f, t) \\ 275 \quad = PA_{lung}(f, t) - mean(PA_{bronchi}(f, t)) \quad (2)$$

276 F. DATA ANALYSIS

277 For tissue differentiation analysis among non-smoker, smoker
278 and ex-smoker samples in healthy lung tissue samples as well
279 as for tissue differentiation analysis between healthy lung
280 tissue and neoplasm lung tissue the averaged spectra of the
281 bioimpedance measurements, obtained using the 3-electrode
282 method, throughout the acquisition time was used.

283 The frequency range chosen to visualize and analyze
284 the data was 15 kHz – 307 kHz. The values from fre-
285 quencies higher and lower than this range were discarded
286 due to electrode effects at low frequency and capacitive
287 coupling errors at high frequency. For tissue differentia-
288 tion analysis the frequency of 15 kHz for |Z| and R and
289 the frequency of 307 kHz for PA and Xc were chosen.
290 These frequencies were chosen based on the higher distance
291 between the means of the groups used to perform the tissue
292 differentiation.

293 The normality of the distribution of the variables was
294 determined by the Kolmogorv-Smirnov (healthy lung tissue
295 samples) test and Shapiro-Wilk test (neoplasm lung tissue
296 samples). The variables normally distributed are shown as the
297 mean \pm standard deviation (SD) and 95% confidence interval
298 (CI) for the mean (lower bound and upper bound). Non-
299 normally distributed variables are shown as statistic median
300 (interquartile range, IQR) and minimum - maximum. One-
301 way analysis of variance (ANOVA) was used to determine
302 statistically significant differences in the |Z|, PA, R and Xc
303 values among smokers, non-smokers and ex-smoker samples
304 in healthy lung tissue. Repeated measures t-test was used to
305 determine statistically significant differences in the |Z|, PA,
306 R and Xc values between non-calibrated data and calibrated
307 data among smokers, non-smokers and ex-smoker healthy
308 lung samples. One-way analysis of variance (ANOVA, para-
309 metric data) and Mann–Whitney U test (non-parametric data)
310 was used to determine statistically significant differences in
311 the |Z|, PA, R and Xc values between healthy lung tissue
312 and neoplasm lung tissue. In addition, the area under the
313 Receiver Operating Characteristic (ROC) curve was used to
314 measure the discriminative capacity of the non-calibrated
315 and calibrated measure of |Z|, PA, R and Xc according to
316 tissue classification (1: healthy lung tissue; 2: neoplasm lung
317 tissue) by biopsy. Following the ROC analysis area under
318 curve (AUC) above 0.9 is considered a very good model
319 and AUC above 0.97 it is considered as excellent. A value
320 less than 0.5 indicates the model is no better than random
321 prediction.

322 The statistical software IBM® SPSS® version 28.0 (IBM
323 Corp, Armonk, NY, United States) was used for data analysis.
324 The level of statistical significance was set at $P < 0.05$.

III. RESULTS

A. MULTI-FREQUENCY RESPONSE FOR MINIMALLY INVASIVE HEALTHY LUNG TISSUE MEASUREMENTS

325 Fig. 3 shows the mean (continuous line) and SD (dashed
326 lines) values of |Z|, PA, R and Xc plotted along the fre-
327 quency range (15 kHz – 307 kHz) used for the measures
328 obtained in healthy lung tissue divided in smoker patients
329 (red), non-smokers patients (green) and ex-smoker patients
330 (blue) for non-calibrated (left) bioimpedance measures
331 and calibrated bioimpedance measures (right) showing an inter-
332 sample reduction of the dispersion and increasing data
333 homogeneity.
334
335
336

B. TISSUE DIFFERENTIATION AMONG NON-SMOKERS, SMOKERS AND EX-SMOKERS PATIENTS IN CALIBRATED AND NON-CALIBRATED DATA

337 Table 1 lists the descriptive parameters, specified as the mean
338 \pm SD, 95% confidence interval for mean (lower bound and
339 upper bound) of |Z|, PA, R and Xc and the results of the
340 one-way ANOVA including the Fisher coefficient (F) for
341 the minimally-invasive bioimpedance measures performed
342 in healthy lung tissue (non-smokers: $n = 22$; smokers:
343 $n = 9$; ex-smokers: $n = 23$) for the measures calibrated
344 and non-calibrated. No statistically significant differences
345 ($P > 0.05$) related to the smoking condition are found
346 among the three groups analyzed for both calibrated and non-
347 calibrated
348 data.
349
350
351

C. MULTI-FREQUENCY RESPONSE FOR MINIMALLY INVASIVE HEALTHY LUNG TISSUE AND NEOPLASM LUNG TISSUE MEASUREMENTS

352 Fig. 4 shows the mean (continuous line) and SD (dashed
353 lines) values of |Z|, PA, R and Xc plotted along the frequency
354 range (15 kHz – 307 kHz) used for the measures obtained in
355 healthy lung tissue (green) and neoplasm lung tissue (black)
356 before (left) and after (right) calibration respectively. Results
357 show an increase in the separation between tissues in |Z|,
358 R and Xc, especially the first two.
359
360
361

D. TISSUE DIFFERENTIATION BETWEEN HEALTHY LUNG TISSUE AND NEOPLASM LUNG TISSUE

362 Table 2 lists the descriptive parameters, specified as the mean
363 \pm SD, 95% confidence interval for mean (lower bound and
364 upper bound) for normally distributed variables and specified
365 as statistic median (interquartile range, IQR) and minimum –
366 maximum for non-normally distributed variables of |Z|, PA,
367 R and Xc and the results of the one-way ANOVA including
368 the Fisher coefficient (F) and the Mann–Whitney U test
369 results including the U statistic (U) for the minimally invasive
370 bioimpedance measures performed in healthy lung tissue
371 ($n = 54$) and in neoplasm lung tissue ($n = 15$) for
372 the measures calibrated and non-calibrated. Statistically
373 significant differences ($P < 0.001$) are found between
374
375

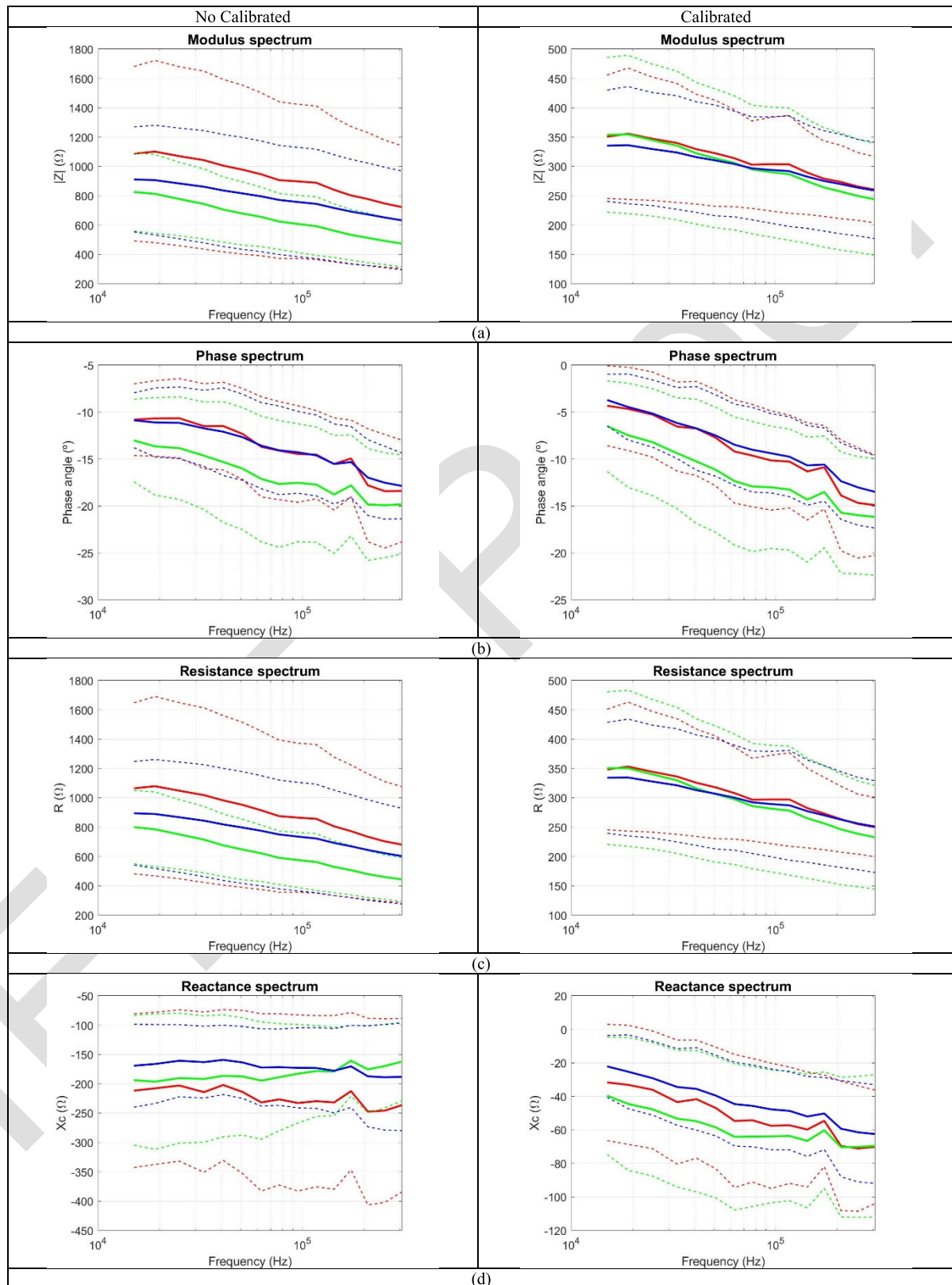


FIGURE 3. Results of the non-calibrated (left) and calibrated (right) mean (continuous line) and SD (dashed lines) parameters extracted from the bioimpedance signal along the different frequencies analyzed (15 kHz – 307 kHz). In order, (a) Modulus, (b) Phase angle, (c) Resistance and (d) Reactance of the bioimpedance of all the different measures taken in healthy lung tissue classified according to cigarette consumption. Green: non-smoker; blue: ex-smokers; red: smokers.

TABLE 1. Descriptions of bioimpedance measurements performed in healthy lung tissue for non-smokers, smokers and ex-smokers. The variables normally distributed are shown as mean \pm SD, 95% confidence interval for mean (lower bound and upper bound). In addition, the Fisher (F) coefficient for variance analysis and the statistical significance (P) are also shown.

No calibrated data					
	Mean \pm SD 95% CI (lower bound – upper bound)			F	P
	Non-smokers (n = 22)	Smokers (n = 9)	Ex-smokers (n = 23)		
Z (Ω)	670.99 \pm 308.96 (433.51 - 908.48)	1086.97 \pm 594.40 (630.07 - 1543.86)	1016.66 \pm 492.09 (638.40 - 1394.92)	1.523	0.228
PA ($^\circ$)	-17.47 \pm 6.77 (-22.68 – (-12.27))	-18.40 \pm 5.41 (-22.56 – (-14.24))	-17.56 \pm 4.08 (-20.70 – (-14.42))	1.000	0.375
R (Ω)	649.35 \pm 289.72 (426.65 - 872.05)	1064.34 \pm 583.33 (615.95 - 1512.72)	997.28 \pm 487.75 (622.36 - 1372.20)	1.646	0.203
Xc (Ω)	-116.62 \pm 64.24 (-166.00 – (-67.24))	-236.36 \pm 147.90 (-350.05 – (-122.68))	-203.36 \pm 115.60 (-292.22 – (-114.50))	1.929	0.156
Calibrated data					
	Mean \pm SD 95% CI (lower bound – upper bound)			F	P
	Non-smokers (n = 22)	Smokers (n = 9)	Ex-smokers (n = 23)		
Z (Ω)	298.72 \pm 107.35 (216.21 - 381.24)	350.61 \pm 105.20 (269.74 - 431.47)	304.16 \pm 86.61 (237.58 - 370.74)	0.156	0.856
PA ($^\circ$)	-14.88 \pm 8.01 (-21.04 – (-8.72))	-14.91 \pm 5.34 (-19.01 – (-10.81))	-12.53 \pm 5.02 (-16.38 – (-8.67))	1.422	0.881
R (Ω)	296.07 \pm 105.24 (215.18 - 376.96)	348.24 \pm 102.79 (269.23 - 427.25)	302.71 \pm 85.53 (236.96 - 368.46)	0.127	0.881
Xc (Ω)	-50.69 \pm 30.68 (-74.27 – (-27.11))	-70.10 \pm 33.83 (-96.11 – (-44.10))	-50.20 \pm 22.79 (-67.72 – (-32.69))	0.255	0.776

376 healthy and neoplasm lung tissue for both calibrated and
377 non-calibrated data.

378 E. EFFECTS OF CALIBRATION IN DATA VARIABILITY IN 379 HEALTHY LUNG TISSUE AND IN NEOPLASM LUNG TISSUE

380 Fig. 5 shows the effect of calibration in bioimpedance data
381 variability for healthy lung tissue and neoplasm lung tissue
382 respectively for |Z| and R at 15 kHz and for PA and Xc at
383 307 kHz. Results show a decrease in data dispersion within
384 the same tissue group, especially in |Z| and R parameters,
385 after the calibration of the bioimpedance data. Fig. 6 shows
386 the receiver operating characteristic (ROC) curves for |Z|, PA,
387 R and Xc before and after calibration for healthy lung tissue
388 and neoplasm lung tissue groups. Results show an increase
389 of the area under curve (AUC) after the calibration of the
390 bioimpedance data in |Z|, R and Xc (AUC > 0.96) and a
391 decrease of the AUC in PA (AUC < 0.95).

392 IV. DISCUSSION

393 This project evaluates the need of the calibration of the
394 minimally invasive EIS bioimpedance measures performed
395 in lung tissue using a measure performed in bronchial tissue.
396 Moreover, it evaluates the influence of cigarette smoking
397 in healthy lung tissue bioimpedance measures as a possible
398 cause of dispersion. Finally, it differentiates between healthy
399 and neoplasm lung tissue and assesses the possible improve-
400 ment of this differentiation using the calibration.

Lungs are organs that belong to the respiratory system
whose principal function is to produce gas exchange. Structures
from the respiratory system include trachea, bronchi and
terminal bronchioles. Each of these structures has its own
anatomical and histological characteristics [19]. Therefore,
differences in bioimpedance measurements can be expected
based not only on the type of tissue but also on its state.

This work reports the use of minimally invasive EIS in
lungs through a bronchoscopy process using the 3-electrode
method to differentiate among smoker, non-smokers and
ex-smoker healthy lung tissue samples, in order to analyze
its potential role in the measurements variability and to differ-
entiate between healthy lung tissue and neoplasm lung
tissue. Both tissue differentiations are used to evaluate the
inter-patient variability in the mentioned groups and to eval-
uate the utility of calibration using a bioimpedance measure
performed in a principal bronchus. This strategy of taking a
measure to calibrate the other measures has been previously
used in heart applications [18].

The inflammatory response due to cigarette consumption
is not differentiable through bioimpedance EIS measures
neither with the non-calibrated measurements nor with the
calibrated measures. Therefore, the initial hypothesis that
the smoking condition could be a cause of dispersion in the
EIS-derived estimators can be discarded. According to Fig. 3
the |Z| and R show a decrease in their values when calibrating
with respect to a bronchi measurement while PA and Xc
increase their values (nearer to 0 than the non-calibrated

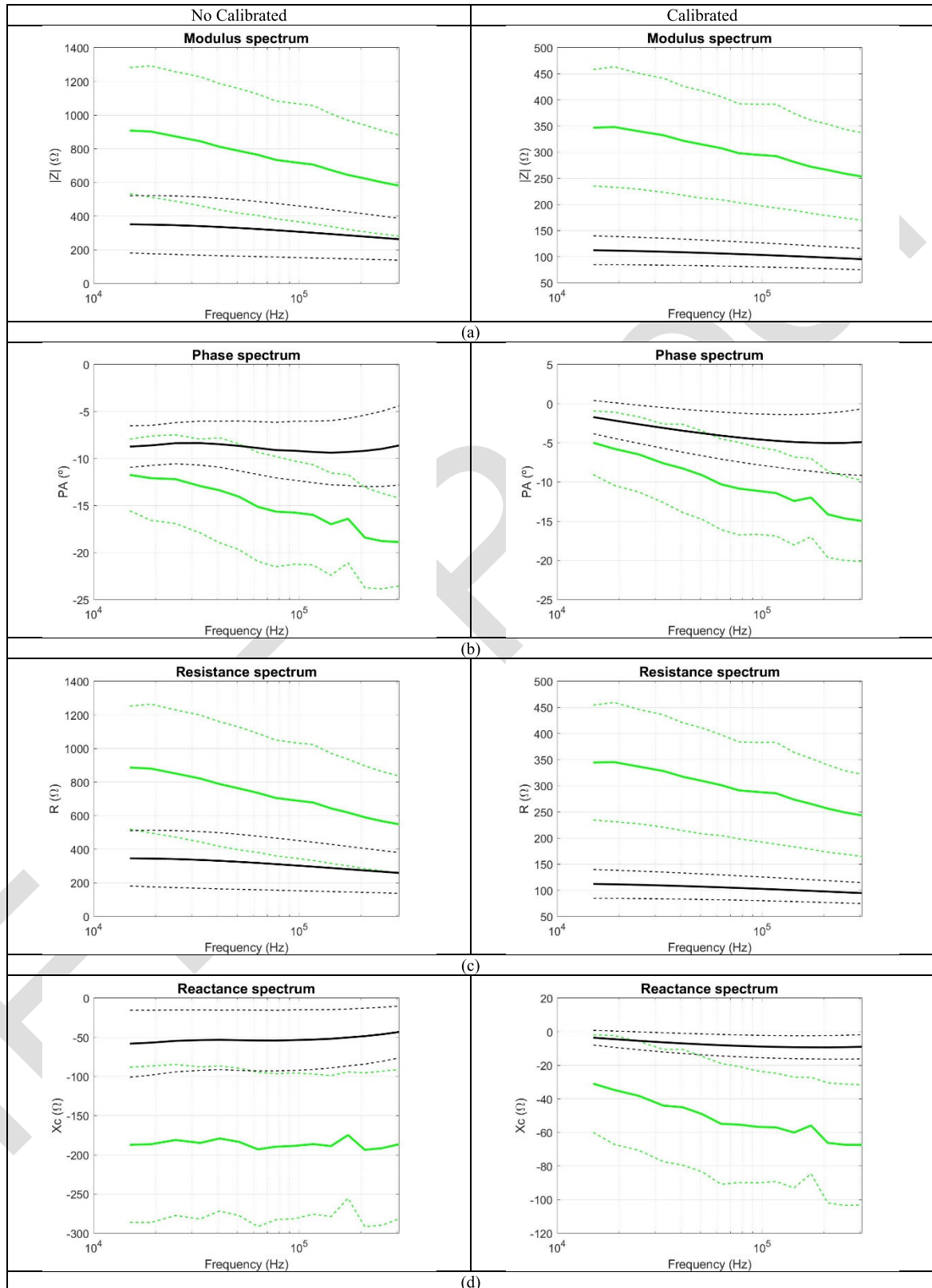


FIGURE 4. The mean (continuous line) and SD (dashed lines) values from the bioimpedance signal along the different frequencies analyzed before and after calibration. The (a) modulus, (b) phase angle, (c) resistance and (d) capacitive reactance. Green: healthy lung tissue; black: neoplasm lung tissue.

TABLE 2. Descriptions of minimally-invasive bioimpedance measurements for healthy lung tissue and neo-plasm lung tissue. The variables normally distributed are shown as mean \pm SD, 95% confidence interval for mean (lower bound and upper bound) while that non-normally distributed data are shown as statistic median (interquartile range, IQR) and minimum-maximum. In addition, the statistic of the Mann Whitney U test (U), the Fisher (F) coefficient for variance analysis and the statistical significance (P) are also shown.

	No calibrated data				Calibrated data			
	Healthy (n = 54)	Neoplasm (n = 15)	U	P	Healthy (n = 54)	Neoplasm (n = 15)	F	P
Z (Ω)	751.97 (759.66) (305.85 - 1823.16)	284.95 (308.09) (134.68 - 668.53)	44	<0.001	283.26 \pm 80.68 (238.58 - 327.94)	112.38 \pm 27.56 (97.12 - 127.65)	64.735	<0.001
PA ($^\circ$)	-15.98 \pm 5.60 (-19.08 - (-12.88))	-8.61 \pm 4.21 (-10.94 - (-6.28))	36	<0.001	-11.61 \pm 5.21 (-14.49 - (-8.72))	-4.90 \pm 4.24 (-7.25 - (-2.55))	47.597	<0.001
R (Ω)	741.72 (731.03) (303.32 - 1799.63)	283.41 (302.44) (133.39 - 650.79)	44	<0.001	281.77 \pm 79.71 (237.63 - 325.91)	112.26 \pm 27.51 (97.02 - 127.49)	65.099	<0.001
Xc (Ω)	-146.04 (139.73) (-405.34 - (-21.95))	-43.17 \pm 33.05 (-61.48 - (-24.87))	39	<0.001	-44.46 \pm 22.51 (-56.92 - (-31.99))	-8.97 \pm 7.18 (-12.94 - (-4.99))	39.142	<0.001

data). The non-calibrated |Z| and R as well as the PA show slightly although non-significative higher values in those samples in which cigarette consumption is present. However, Xc present lower values in smoker samples. When we calibrate the bioimpedance measurements we show an intra-sample variability reduction. This variability reduction specially affects |Z| and R due to the geometrical dependence of R and the high correlation between |Z| and R [5], [6].

Emphasizing the importance of the analysis of R and Xc according to the theory of Lukaski *et al.* [6], [7], Piccoli *et al.* [20], and Lukaski *et al.* [21] we selected the frequencies (15 kHz and 307 kHz) to check the hypothetical differentiation among non-smokers, smokers and ex-smokers healthy lung tissue samples following the calculation of the maximum distance between means of the three groups. From the bioimpedance parameters, R describes the behavior of the medium through which the current flows while Xc describes the capacitive component of the cell membranes. The values of |Z| and PA are dependent of R and Xc [6], [7].

The significance of the test was determined with the p-value which is the probability of obtaining test results at least as extreme as the result observed, assuming that the null hypothesis is correct. Therefore, considering the level of significance set, results will be statistically significant if a $P < 0.05$ is obtained in the test. Regarding tissue differentiation among non-smokers, smokers and ex-smokers healthy lung tissue samples, one-way ANOVA reported non-significant results ($P > 0.05$) for all variables (|Z|, PA, R and Xc) for both, the non-calibrated and the calibrated measures. No post-hoc test has been done as no significant results have been found. The Fisher coefficient parameter (F) represents the relationship between the inter-group variance and the intra-group variance. Therefore, a higher F coefficient indicates a higher inter-group variance than intra-group variance [22]. According to the results obtained in **Table 1**, the F coefficient obtained in the non-calibrated data is higher in |Z|, R and Xc than in the calibrated data. In contrast, F coefficient in PA obtained in the calibrated data is higher than in the non-calibrated data. Therefore, the statistical results obtained show that the effect of cigarette consumption should not be considered to perform tissue differentiation

through bioimpedance analysis. Moreover, results show an intra-sample dispersion reduction with the effect of calibration, especially in |Z| and R, which depend on the geometrical factors.

Regarding tissue differentiation between healthy lung tissue and neoplasm lung tissue we have taken all the healthy lung tissue samples without considering the tabaco habits as it has been demonstrated that this factor is not significant ($P > 0.05$). Lung cancer is a highly complex neoplasm and comprise several histological types. The groups most frequently are the non-small cell lung cancer (NSCLC) such as adenocarcinoma and squamous carcinoma, followed by small cell lung cancer (SCLC) [23]. Lung cancer are the results of the accumulation of genetic and epigenetic changes, including abnormalities of the inactivation of tumour-suppression genes and the activation of oncogenes [24]. For the tissue differentiation between healthy lung tissue and neoplasm lung tissue all cancer types have been included in the same group so we assume that the remaining dispersion in neoplasm lung tissue might be due to the differences within lung cancer types. We have selected the frequencies (15 kHz and 307 kHz) that offered us a better discriminatory response between healthy lung tissue and neoplasm by taking the frequency with the maximum difference between the mean of the healthy lung tissue and the mean of the neoplasm lung tissue. We have also visualized the mean impedance spectrum and SD of the healthy lung tissue samples and the neoplasm lung tissue samples between the frequency range analyzed (15 kHz – 307 kHz) with the data non-calibrated and calibrated to show the effects of the calibration. According to the results obtained in **Fig. 4** the calibration of the bioimpedance measures with respect to a measure performed in bronchi reduces the intra-group variability and, in consequence, increases the inter-patient distance in both, the healthy lung tissue and the neoplasm lung tissue, especially in |Z| and R, which are the two parameters that are dependent on geometrical factors (**Fig. 5**). Results obtained show a higher |Z| and R and a lower PA and Xc in healthy lung tissue than in neoplasm lung tissue. Moreover, |Z| and R show higher difference between the lower frequencies and the higher frequencies in healthy lung tissue than in neoplasm lung tissue.

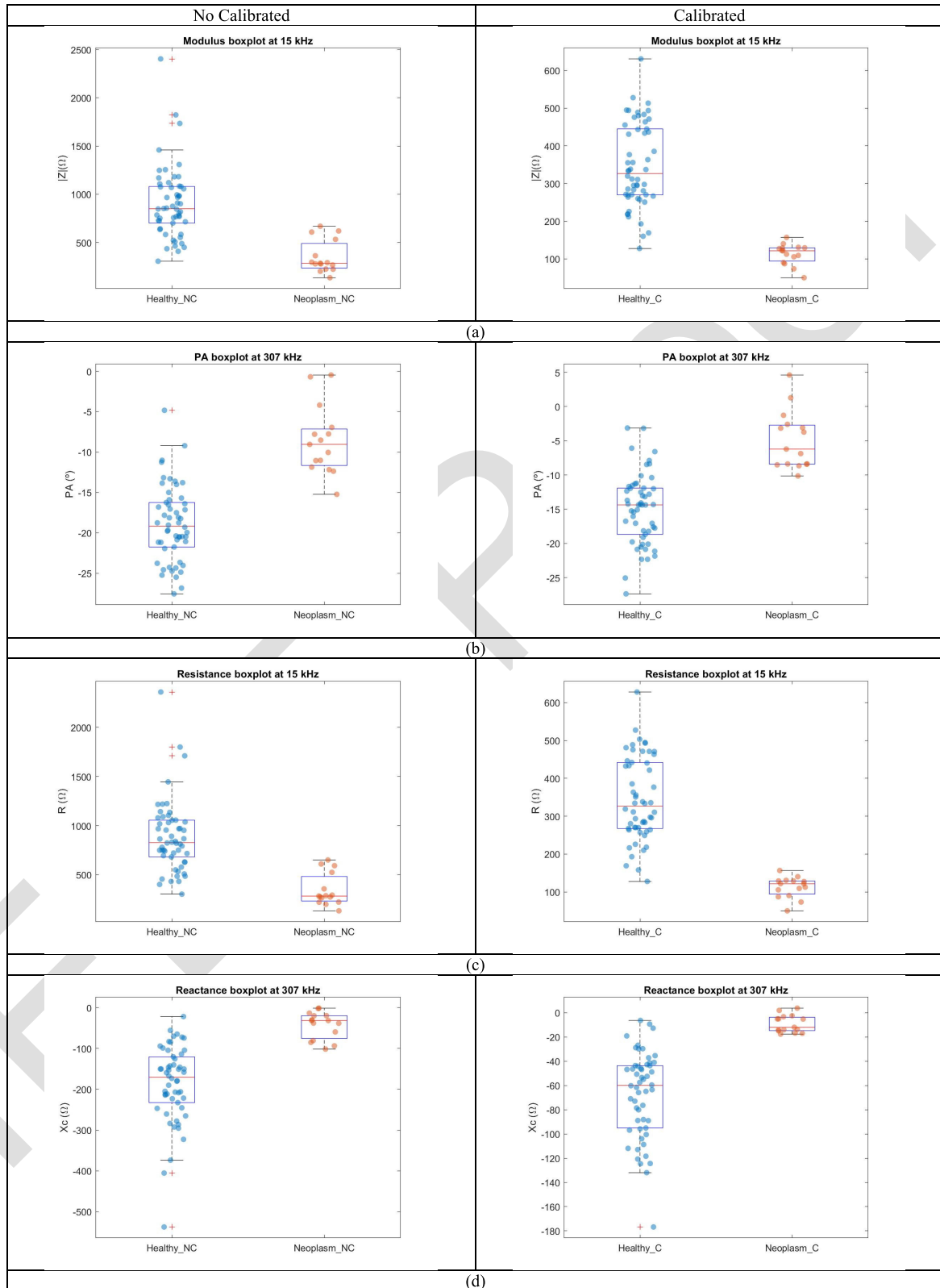


FIGURE 5. Boxplot of bioimpedance calibrated (C) and non-calibrated (NC) data of healthy lung tissue and neoplasm lung tissue for (a) $|Z|$ and (c) R at 15 kHz and for (b) PA and (d) X_c at 307 kHz. The central mark of each box indicates the median, and the bottom and top edges of the box indicate the 25th and 75th percentiles, respectively. The whiskers extend to the most extreme data points that are not considered outliers. In addition, the bioimpedance data values for the calibrated (blue) and non-calibrated (orange) measures. Vertical axis are different for the calibrated and non-calibrated data for better data visualization.

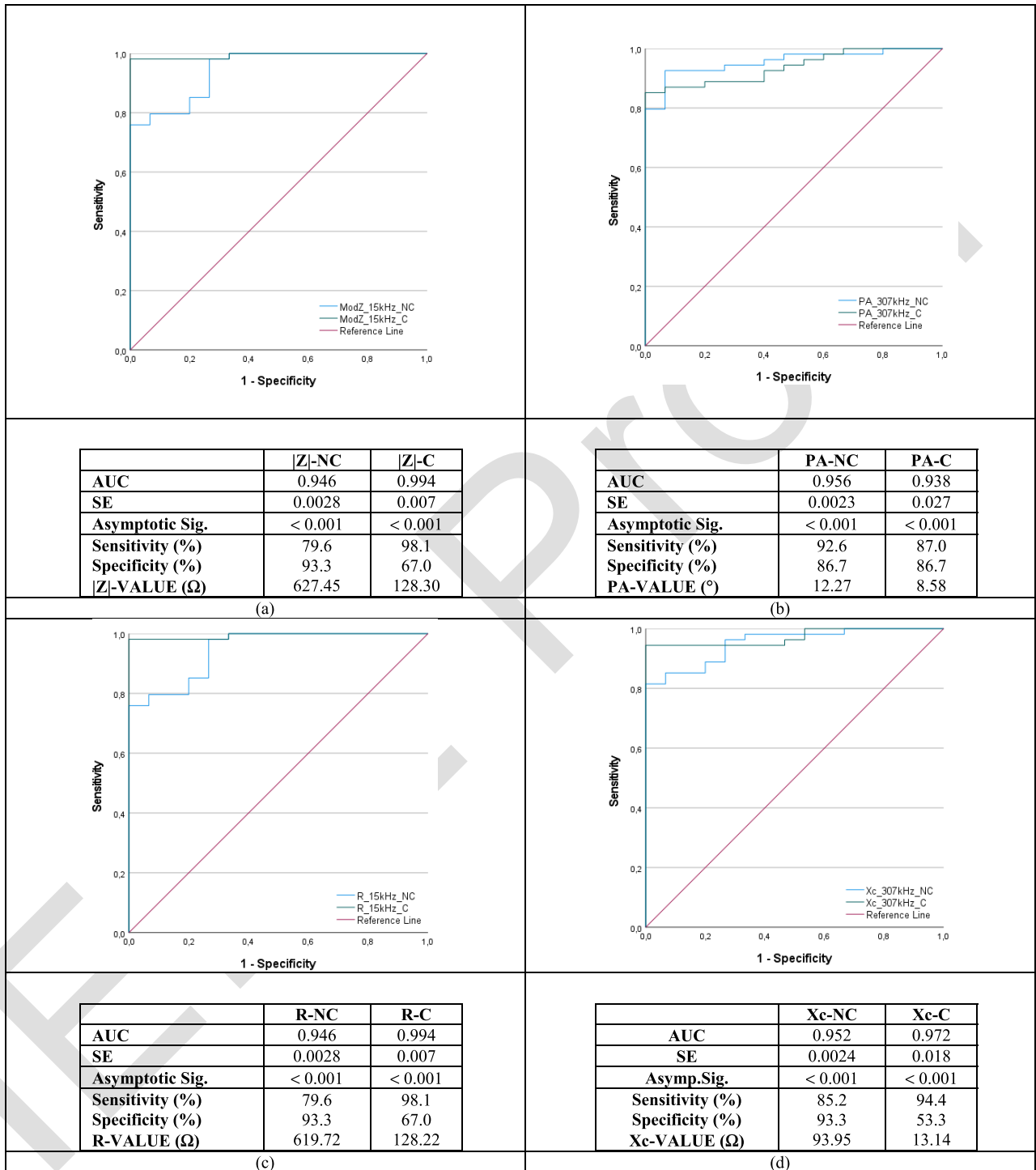


FIGURE 6. Receiver operating characteristic (ROC) curves to assess the predictive ability of the different electrical impedance parameters before and after calibration between healthy and neoplasm lung tissue. In (a) the results of the $|Z|$ before calibration (NC) and after calibration (C) at 15 kHz. In (b) the results of the PA before calibration (NC) and after calibration (C) at 307 kHz. In (c) the results of the R before (NC) and after (C) calibration at 15 kHz. In (d) the results of the Xc before (NC) and after (C) calibration at 307 kHz.

511 EIS assumes that current at low frequency flows through the
 512 extracellular space while current at high frequencies flows
 513 through both, intracellular and extracellular space. Moreover,
 514 healthy lung tissue is composed of alveolar epithelial and

515 endothelial cells separated by a thin basement membrane
 516 and interstitial space. Interstitial space is a non-conductive
 517 medium, than the neoplasm lung tissue. These two main char-
 518 acteristics produce a higher $|Z|$ and R in healthy lung tissue

519 than in neoplasm lung tissue. Lung cancer produce multi-
 520 ples histological changes of the normal bronchial mucosa.
 521 Proliferation of epithelial cells with abundant cytoplasm and
 522 vesicular nuclei, intercellular bridging, thickening of alveolar
 523 septa and others pathological changes [25]. The morphologic
 524 features in neoplasm lung tissue seem to contribute to lose
 525 their capacitive behavior which is translated into a PA and
 526 Xc flat mean impedance spectrum, as compared to the healthy
 527 lung tissue mean impedance spectrum (**Fig. 4**). Regarding tis-
 528 sue differentiation between healthy lung tissue and neoplasm
 529 lung tissue, one-way ANOVA for the calibrated data and
 530 Mann–Whitney U test for the non-calibrated data (**Table 2**)
 531 show statistically significant differences between the two
 532 groups (healthy and neoplasm lung tissue, $P < 0.001$). These
 533 statistical differences are probably due to the histological
 534 differences between both groups by minimally-invasive EIS
 535 measurements. Focusing only in the calibrated data results
 536 in **Table 2** show higher significance in $|Z|$ and R than in
 537 PA and Xc as the F coefficient is higher in the first two
 538 parameters.

539 The study has shown that there is an effect on the mea-
 540 surement when calibrating, reducing the dispersion of the
 541 measurements (**Fig. 5**). Calibration doesn't change the out-
 542 come of the hypothesis test, showing a statistically significant
 543 difference in both cases, but the higher-F coefficient (Fisher
 544 coefficient from one-way ANOVA test, used for comparing
 545 the factors of the total deviation) than U (statistic from
 546 Mann–Whitney U test, used to assess whether two sampled
 547 groups are likely to derive from the same population) suggests
 548 stronger separation between the groups (**Table 2**), which is
 549 highly significant ($P < 0.01$) for both calibrated and non-
 550 calibrated measures. On the other hand, according to the ROC
 551 curve analysis, (**Fig. 6**) we have observed that the area under
 552 the curve (AUC) is equally excellent in all the variables (AUC
 553 > 0.9) both calibrating and not calibrating, although higher
 554 AUC values are observed when calibrating. After calibrating,
 555 the AUC is greater than 0.96 for all cases except in PA.
 556 The $|Z|$, R and Xc increase the sensitivity (true positive
 557 fraction) and decrease the specificity (false positive fraction)
 558 after calibration. Only PA showed a decrease in sensitivity
 559 maintaining its specificity (**Fig. 6**). Considering that PA has
 560 a trigonometric relationship between R and Xc and that these
 561 improve with calibration, the authors recommend perform-
 562 ing the calibration of the measurements with respect to the
 563 bronchi.

564 In the previous study performed by Company-Se et al. [14]
 565 we performed tissue differentiation between healthy lung
 566 tissue and bronchi tissue. We proposed continuing with
 567 the study by including neoplasm lung tissue for lung
 568 tissue differentiation. Results obtained in **Table 2** show
 569 that minimally invasive electrical impedance spectroscopy
 570 using the 3-electrode method is able to discriminate with
 571 both, calibrated data (not considering geometrical factors)
 572 and with non-calibrated data. In future studies we aim
 573 to include other lung pathologies with other histological
 574 characteristics.

575 V. CONCLUSION 576

577 In conclusion, results of the healthy lung tissue bioimpedance
 578 measurements show that there are no significant differences
 579 between healthy lung tissue among smoker, non-smoker and
 580 ex-smoker measures, which was initially stated as a possible
 581 cause of EIS measurement dispersion in lungs. Then, to per-
 582 form tissue differentiation between healthy lung tissue and
 583 neoplasm lung tissue the effect of tobacco habit will not be
 584 considered. Also, this effect will not be considered in our
 585 future studies.

586 On the other hand, we found that there is a statistically
 587 significant difference in both calibrated and non-calibrated
 588 measurements at 15 kHz ($|Z|$ and R) and 307 kHz (Xc and
 589 PA) between healthy and neoplasm lung tissue. This shows
 590 that minimally invasive electrical impedance spectroscopy
 591 measurements using the 3-electrode method are able to dis-
 592 criminate between healthy lung and neoplasm both with and
 593 without calibration.

594 Calibration has, however, been demonstrated to reduce
 595 data variability and increase the tissue state separa-
 596 tion capability, which will be useful in future studies
 597 when including other pathologies with similar pathological
 598 mechanisms.

599 Moreover, significant differences are found between cal-
 600 ibrated and non-calibrated paired samples of smoker, non-
 601 smoker ex-smoker and neoplasm lung tissue showing that
 602 calibration is beneficial to reduce intra-sample variability.

603 The authors recommend calibrating the measures obtained
 604 with respect to the bronchi given that it is demonstrated
 605 that it increases the sensitivity of the 3-electrode mini-
 606 mally invasive electrical impedance spectroscopy for tissue
 607 differentiation.

608 ACKNOWLEDGMENT

609 The authors would like to specially thank the patients
 610 without whom this study would not have been possible.
 611 In addition, they would like to thank Marta Navarro Colom,
 612 Laura Romero Roca, and Margarita Castro Jiménez from
 613 the Interventional Pulmonology Unit, Respiratory Medicine
 614 Department, Hospital de la Santa Creu i Sant Pau for the
 615 invaluable support. Author Contributions: Ramon Bragós,
 616 Virginia Pajares, Pere J. Riu, Javier Rosell, Georgina
 617 Company-Se, Alfons Torrego, and Lexa Nescolarde designed
 618 the experiments; Georgina Company-Se, Virginia Pajares,
 619 and Alfons Torrego performed the experiments; Lexa Nescolarde
 620 and Georgina Company-Se performed the data process-
 621 ing; Lexa Nescolarde, Georgina Company-Se, and Ramon
 622 Bragós analyzed the data; Georgina Company-Se and Lexa
 623 Nescolarde drafted the manuscript and prepared the tables
 624 and figures; and Ramon Bragós, Virginia Pajares, Pere J. Riu,
 625 Javier Rosell, Georgina Company-Se, Alfons Torrego, and
 626 Lexa Nescolarde revised the paper and approved the final
 627 version of the manuscript.

628 REFERENCES

- 629 [1] I. Annesi-Maesano and G. Viegi, Eds., *Respiratory Epidemiology*.
 630 Lausanne, Switzerland: European Respiratory Society, 2014.

- [2] H. J. de Koning, "Reduced lung-cancer mortality with volume CT screening in a randomized trial," *New England J. Med.*, vol. 382, no. 6, pp. 503–513, Feb. 2020, doi: [10.1056/NEJMoa1911793](https://doi.org/10.1056/NEJMoa1911793).
- [3] D. E. Ost, "Diagnostic yield and complications of bronchoscopy for peripheral lung Lesions. Results of the AQUIRE registry," *Amer. J. Respiratory Crit. Care Med.*, vol. 193, no. 1, pp. 68–77, Jan. 2016, doi: [10.1164/rccm.201507-1332OC](https://doi.org/10.1164/rccm.201507-1332OC).
- [4] J. S. Wang Memoli, P. J. Nietert, and G. A. Silvestri, "Meta-analysis of guided bronchoscopy for the evaluation of the pulmonary nodule," *Chest*, vol. 142, no. 2, pp. 385–393, Aug. 2012, doi: [10.1378/chest.11-1764](https://doi.org/10.1378/chest.11-1764).
- [5] S. Khalil, M. Mohktar, and F. Ibrahim, "The theory and fundamentals of bioimpedance analysis in clinical status monitoring and diagnosis of diseases," *Sensors*, vol. 14, no. 6, pp. 10895–10928, Jun. 2014, doi: [10.3390/s140610895](https://doi.org/10.3390/s140610895).
- [6] H. C. Lukaski, N. V. Diaz, A. Talluri, and L. Nescolarde, "Classification of hydration in clinical conditions: Indirect and direct approaches using bioimpedance," *Nutrients*, vol. 11, no. 4, p. 809, Apr. 2019, doi: [10.3390/nu11040809](https://doi.org/10.3390/nu11040809).
- [7] H. C. Lukaski, "Biological indexes considered in the derivation of the bioelectrical impedance analysis," *Amer. J. Clin. Nutrition*, vol. 64, no. 3, pp. 397S–404S, Sep. 1996, doi: [10.1093/ajcn/64.3.397S](https://doi.org/10.1093/ajcn/64.3.397S).
- [8] S. Toso, "Altered tissue electric properties in lung cancer patients as detected by bioelectric impedance vector analysis," *Nutrition*, vol. 16, no. 2, pp. 120–124, Feb. 2000, doi: [10.1016/s0899-9007\(99\)00230-0](https://doi.org/10.1016/s0899-9007(99)00230-0).
- [9] D. M. Nierman, D. I. Eisen, E. D. Fein, E. Hannon, J. I. Mechanick, and E. Benjamin, "Transthoracic bioimpedance can measure extravascular lung water in acute lung injury," *J. Surgical Res.*, vol. 65, no. 2, pp. 101–108, Oct. 1996, doi: [10.1006/jrsr.1996.0350](https://doi.org/10.1006/jrsr.1996.0350).
- [10] J. Orschulik, N. Hochhausen, S. A. Santos, M. Czaplak, S. Leonhardt, and M. Walter, "Detection of acute respiratory distress syndrome using sectoral bioimpedance spectroscopy—A pilot study," in *Proc. 11th Int. Conf. Bioelectromagn.*, Aachen, Germany, May 2018, pp. 1–10. [Online]. Available: <http://publications.rwthachen.de/record/723538/files/723538.pdf>
- [11] B. Sanchez, G. Vandersteen, I. Martin, D. Castillo, A. Torrego, P. J. Riu, J. Schoukens, and R. Bragos, "in vivo electrical bioimpedance characterization of human lung tissue during the bronchoscopy procedure. A feasibility study," *Med. Eng. Phys.*, vol. 35, no. 7, pp. 949–957, Jul. 2013, doi: [10.1016/j.medengphy.2012.09.004](https://doi.org/10.1016/j.medengphy.2012.09.004).
- [12] N. Coll, R. Bragós, A. M. Muñoz, V. Pajares, A. Torrego, and P. J. Riu, (2016). *Espectrometría de Impedancia Eléctrica en Tejido Pulmonar*. [Online]. Available: <https://lupcommons.upc.edu/handle/2117/100980>
- [13] P. J. Riu, G. Company, R. Bragos, J. Rosell, V. Pajares, and A. Torrego, "Minimally invasive real-time electrical impedance spectroscopy diagnostic tool for lung parenchyma pathologies," in *Proc. 42nd Annu. Int. Conf. IEEE Eng. Med. Biol. Soc. (EMBC)*, Jul. 2020, pp. 5077–5080, doi: [10.1109/EMBC44109.2020.9175860](https://doi.org/10.1109/EMBC44109.2020.9175860).
- [14] G. Company-Se, L. Nescolarde, V. Pajares, A. Torrego, P. J. Riu, J. Rosell, and R. Bragos, "Minimally invasive lung tissue differentiation using electrical impedance spectroscopy: A comparison of the 3- and 4-electrode methods," *IEEE Access*, vol. 10, pp. 7354–7367, 2022, doi: [10.1109/ACCESS.2021.3139223](https://doi.org/10.1109/ACCESS.2021.3139223).
- [15] K. Subramaniam, A. R. Clark, E. A. Hoffman, and M. H. Tawhai, "Metrics of lung tissue heterogeneity depend on BMI but not age," *J. Appl. Physiol.*, vol. 125, no. 2, pp. 328–339, Aug. 2018, doi: [10.1152/jappphysiol.00510.2016](https://doi.org/10.1152/jappphysiol.00510.2016).
- [16] S. Weitzman and L. Gordon, "Inflammation and cancer: Role of phagocyte-generated oxidants in carcinogenesis," *Blood*, vol. 76, no. 4, pp. 655–663, Aug. 1990.
- [17] R. O'Donnell, "Inflammatory cells in the airways in COPD," *Thorax*, vol. 61, no. 5, pp. 448–454, May 2006, doi: [10.1136/thx.2004.024463](https://doi.org/10.1136/thx.2004.024463).
- [18] G. Amorós-Figueras, E. Jorge, C. Alonso-Martin, D. Traver, M. Ballesta, R. Bragós, J. Rosell-Ferrer, and J. Cinca, "Endocardial infarct scar recognition by myocardial electrical impedance is not influenced by changes in cardiac activation sequence," *Heart Rhythm*, vol. 15, no. 4, pp. 589–596, Apr. 2018, doi: [10.1016/j.hrthm.2017.11.031](https://doi.org/10.1016/j.hrthm.2017.11.031).
- [19] J. F. Murray, "The structure and function of the lung," *Int. J. Tuberculosis Lung Diseases, Off. J. Int. Union Tuberculosis Lung Diseases*, vol. 14, no. 4, pp. 391–396, Apr. 2010.
- [20] A. Piccoli, B. Rossi, L. Pillon, and G. Bucciante, "A new method for monitoring body fluid variation by bioimpedance analysis: The RXc graph," *Kidney Int.*, vol. 46, no. 2, pp. 534–539, Aug. 1994, doi: [10.1038/ki.1994.305](https://doi.org/10.1038/ki.1994.305).
- [21] K. R. Foster and H. C. Lukaski, "Whole body impedance what does it measure?" *Amer. J. Clin. Nutrition*, vol. 64, no. 3, pp. 388S–396S, Sep. 1996, doi: [10.1093/ajcn/64.3.388S](https://doi.org/10.1093/ajcn/64.3.388S).
- [22] D. F. Morrison, *Multivariate Statistical Methods*. Boca Raton, FL, USA: CRC Press, 1967.
- [23] M. Zheng, "Classification and pathology of lung cancer," *Surgical Oncol. Clinics North Amer.*, vol. 25, no. 3, pp. 447–468, Jul. 2016, doi: [10.1016/j.soc.2016.02.003](https://doi.org/10.1016/j.soc.2016.02.003).
- [24] E. A. Engels, "Inflammation in the development of lung cancer: Epidemiological evidence," *Expert Rev. Anticancer Therapy*, vol. 8, no. 4, pp. 605–615, Apr. 2008, doi: [10.1586/14737140.8.4.605](https://doi.org/10.1586/14737140.8.4.605).
- [25] W. D. Travis, "International association for the study of lung cancer/american thoracic society/European respiratory society international multidisciplinary classification of lung adenocarcinoma," *J. Thoracic Oncol.*, vol. 6, no. 2, pp. 244–285, Feb. 2011, doi: [10.1097/JTO.0b013e318206a221](https://doi.org/10.1097/JTO.0b013e318206a221).



GEORGINA COMPANY-SE received the B.S. degree in biomedical engineering from the Universitat Politècnica de Catalunya (UPC), Barcelona, Spain, in 2018, and the M.S. degree in computational biomedical engineering from Universitat Pompeu Fabra (UPF), Barcelona, in 2019. She is currently pursuing the Ph.D. degree in biomedical engineering with UPC. Her research interests include bioimpedance measures and analysis, signal processing, and data science. She is interested

in machine learning and data science.



LEXA NESCOLARDE was born in Baracoa, Cuba, in 1970. She received the Ph.D. degree in biomedical engineering from the Universitat Politècnica de Catalunya (UPC), Barcelona, Spain, in 2006, under supervision of Professor Javier Rosell. Since January 2001, she has been a member of the Electronic and Biomedical Instrumentation Group (IEB) as well as the Biomedical Research Center (CREB-UPC). She is currently an Associate Professor at UPC. Since 2002, she has been participating in 22 research projects and has led three research and technology transfer contracts of special relevance and two of which are still valid. Her current research interests include use of non-invasive localized bioimpedance measurement (L-BIA) for muscle assessment in high performance athletes, body composition analysis, and data analysis.



VIRGINIA PAJARES was born in Girona, in 1979. She received the Ph.D. degree in medicine and surgery from the Universitat Autònoma de Barcelona, in 2015. She has been a Medical Doctor and a Respiratory Specialist, since 2008. Moreover, she is a Consultant with the Department of Respiratory, Hospital de la Santa Creu i Sant Pau, Barcelona. She is part of the Bronchoscopy Unit Staff and also she works as a Respiratory Residents' Mentor. On 2021, she is author of 20 scientific articles in PubMed. Her main research interests include interventional pulmonology, lung cancer, and pleural diseases.

756
757
758
759
760
761
762
763
764
765
766
767
768



ALFONS TORREGO was born in Barcelona, Spain, in 1971. He has been a Medical Doctor and a Respiratory Specialist, since 2000, and a Consultant with the Department of Respiratory, Hospital de la Santa Creu i Sant Pau, Barcelona. He is also the Bronchoscopy Unit Coordinator at the Hospital de la Santa Creu i Sant Pau. Moreover, he is an Associated Professor of medicine at the Universitat Autònoma de Barcelona and a Former Chairman of the Spanish Respiratory Society Scientific Committee. On 2021, he is author of more than 60 scientific articles in PubMed. His main research interests include interventional pulmonology, lung cancer, and severe asthma.

AQ:5

769
770
771
772
773
774
775
776
777
778
779
780
781
782
783
784
785
786



PERE J. RIU (Senior Member, IEEE) received the M.Sc. degree in telecommunication engineering and the Ph.D. degree in electronic engineering from the Universitat Politècnica de Catalunya (UPC), Barcelona, Spain, in 1986 and 1991, respectively. He was a Visiting Associate Professor with the Department of Bioengineering, University of Pennsylvania, Philadelphia, PA, USA, in 1997. He is currently a Full Professor of electronics with the Department of Electronic Engineering, UPC. His research interests include electromagnetic compatibility, computational electromagnetics, interaction of EMF with biological tissues, and biomedical instrumentation design with emphasis on electrical bioimpedance techniques, including EIT. These activities are performed within the Centre for Research on Biomedical Engineering (CREB, UPC) and the Institut de Recerca Sant Joan de Déu (IRSJD). He is a member of the Committee on Man and Radiation (COMAR) (IEEE-BMES) and the Vice-President of the International Society for Electrical Bio-Impedance.



JAVIER ROSELL (Senior Member, IEEE) was born in Barcelona, Spain, in June 1959. He received the Ingeniero de Telecomunicación and Doctor Ingeniero de Telecomunicación degrees from the Polytechnic University of Catalonia (UPC), Barcelona, in 1983 and 1989, respectively.

He is currently a Full Professor with the Department of Electronic Engineering, UPC, and the Head of the Research Group, Biomedical Research Center (CREB-UPC). His current research interests include non-invasive and non-obtrusive measurement methods in sports, medical and biological fields, particularly based on bio-electrical impedance spectroscopy and magnetic induction spectroscopy.

AQ:6

787
788
789
790
791
792
793
794
795
796
797
798
799
800



RAMON BRAGÓS received the degree in electrical engineering (major in telecommunications engineering) and the Ph.D. degree in electronic engineering from the Technical University of Catalonia (UPC), in 1991 and 1997, respectively. Since 1998, he has been an Associate Professor at the Department of Electronic Engineering, UPC. He belongs to the Electronic and Biomedical Instrumentation Research Group and the Center for Research in Biomedical Engineering (CREB).

His main research interests include design of methods and systems for the characterization of biological materials and systems using minimally invasive methods, mainly electrical impedance spectroscopy.

801
802
803
804
805
806
807
808
809
810
811
812
813
814

• • •